The Effect of Polymer Additives on the Performance of a Two-Roll Coater

YAO-TING KANG, KWONG-YANG LEE, and TA-JO LIU*

Department of Chemical Engineering, National Tsing Hua University, Hsinchu, Taiwan 30043, Republic of China

SYNOPSIS

The effect of polymer additives on the performance of a two-roll coater has been examined experimentally. The coater consists of a rigid steel roll and a deformable roll with polyurethane surface. Newtonian coating solutions and solutions with polymer additives were used as test fluids. Both forward and reverse coating operations were studied. It was found that for the forward coating operation, the shear-thinning behavior of the polymer solutions can reduce the coating thickness, but the fluid elasticity can increase the coating thickness significantly and can also destabilize the coating flow. For the reverse coating operation, a small amount of polymer additives can effectively increase the wipe ratio.

INTRODUCTION

Coating operations have wide industrial applications. Studies on coating flows that are of fundamental and practical importance were reviewed in detail by Ruschak.[1] Among various coating methods, the roll coating operation appears to be a simple and flexible means for depositing a liquid film on a moving substrate. Rolls with different surface characteristics, such as rigid metal rolls, deformable rubber rolls, and gravure rolls with lined or dented surfaces, are frequently used.[2]

Several rolls are usually combined to produce a coating film of desired thickness in practice. However, research works on roll coating are generally focused on the interaction between two rolls. Depending on the direction of rotation between the two rolls under consideration, the roll coating operation can be divided into forward coating, i.e., the two rolls are moving in the same direction in the nip region, or reverse coating, which implies that the two rolls are moving in opposite directions in the nip region.

Most previous research works on roll coating were focused on forward coating operation with two rigid rolls,[3-19] besides studying the coating thickness as functions of fluid properties and operating variables, the upper limit of uniform coating was also analyzed; above this limit, lateral waves on the surface of coated film would appear, the phenomenon of the appearance of lateral waves is called "ribbing." Only recently did several authors analyze the reverse coating flows; they still considered the coating system with two rigid rolls.[20-22] As for coating with deformable rolls, Coyle carried out both theoretical and experimental studies to determine the coating thickness for a forward coating system,[23,24] Newtonian solutions were considered and the two rolls had the same speed in his work.

Polymers are often added to coating solutions, and, owing to these polymer additives, the rheological properties of the solutions may vary significantly. Gutoff and Kendrick[25] found that a small amount of polymer can help stabilize the coating bead and increase the upper limit of coating speed for slide coating. Similar results were found by Lee for an extrusion coating operation.[26] However, Bauman et al. studied the effect of polymer additives on a forward roll coating system and concluded that the fluid elasticity was a destabilizing factor for coating flow.[13] Therefore, depending on the coating system, polymer additives may have stabilizing or destabilizing effects.

In this paper we shall examine how polymer additives would influence the roll coating operation, particularly the coating thickness and the onset of

---

ribbing. A two-roll coater which consists of a rigid metal roll and a deformable roll was used in the experiment. Both forward and reverse coatings were studied in our work.

EXPERIMENTAL

The experimental two-roll coater is shown in Figure 1. The two rolls are replaceable and are driven by separate motors so that the direction of rotation can be altered. Therefore, it is easy for us to perform both forward and reverse coating experiments. The rigid roll is made of stainless steel with a chrome-plated surface, and the deformable roll has a polyurethane (PU) cover of 1 cm thickness. Two PU materials, with hardness Shore A 60 and 90, were selected as covers. An Instron 4201 machine was used to determine the Young's modulus of these two materials. Following the ASTM D-412 Die C test procedure, i.e., maximum load 40 kg and grip rate 500 mm/min, values of the Young's modulus for the two materials were found to be 5.6 and 16.2 MPa, respectively. All the rolls have the same diameter and width, which are 20 and 30 cm, respectively.

The rotational speeds of the rolls were detected by the two digital tachometers attached to the rolls. The range of rotation for these two rolls was between 3 and 150 rpm, with 0.1 rpm errors. A dual-cavity T-die was used to deliver a uniform liquid film on the roll for reverse coating experiment. The performance of this T-die was checked by the design principles of Lee and Liu[27] so that the lateral uniformity of the liquid film could be assured.

To perform the coating experiments, the deformable roll R_2 is pressed on the rigid roll R_1 and the degree of deformation is indicated by a deflection length H_0. For the forward coating system in Figure 1(a), the rigid roll picks up the coating solution from the pan, and the solution will pass through the nip region and spread on both rolls; we can measure the thickness of coated films on both rolls. Then the liquid films are removed by doctor blades and returned to the pan. As for the reverse coating system in Figure 1(b), we use a T-die to deliver a fixed amount of coating solution onto the deformable roll R_2; the solution emanating from the T-die forms a uniform liquid layer on R_2, and then this layer will be passed onto the surface of the rigid roll R_1. The coating thickness on R_1 can be measured, and then the liquid film is removed by a doctor blade and is returned to the pan. Since the deformable roll is pressed on the rigid roll, only a trace of coating solution can pass through the nip region and the
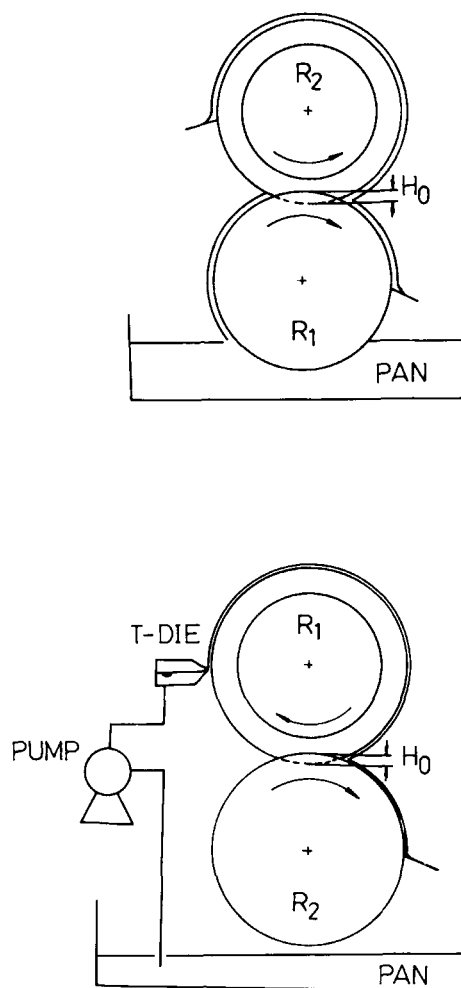
Figure 1 The experimental setup for (a) forward coating and (b) reverse coating.

amount of coating solution remaining on the deformable roll is negligible.

Since the coated film on the rolls can be very thin, it is difficult to measure the coating thickness on the roll surface directly and accurately. We can only determine the average coating thickness by removing the coating solution from the roll within a certain period of time, weigh it, and then compute the average coating thickness.

The following test liquids and polymer additives were used in the experiment:

(a) Silicon oil, made by Toshiba Co.: Samples with five viscosities were used as standard Newtonian test fluids.

(b) Polyisobutylene (PIB), made by Exxon Chemical Co.: code no., Vistanex MML-140; molecular weight (MW): $\sim 2.4 \times 10^6$.

(c) Polybutene (PB), made by Amoco Co. Two

types were used: (i) L-100, MW = 460; (ii) H-300, MW = 1300.

(d) Decalin, Riedel deHaen Co.: code no.: 24219; MW = 138.25.

Kerosene, glycerine, and carboxylmethyl cellulose (CMC, technical grade) were also needed in preparing test solutions. In addition to the silicone oil, four coating solutions were prepared with the materials listed above, and their compositions in terms of weight percentage are given as follows:

(i) 0.12% CMC/water/glycerin:

Weight ratio (WR) = 0.0012/0.1498/0.849

(ii) 2% PIB/kerosene/decalin:

WR = 0.02/0.1125/0.8675

(iii) 0.77% PIB/kerosene/PB(L-100 + H-300):

WR = 0.0077/0.1243/(0.620 + 0.248)

(iv) 4% decalin/PB(L-100 + H-300):

WR = 0.04/(0.686 + 0.274)

To make the two coating solutions with PIB, PIB had to be dissolved in kerosene first, and then mixed with other materials.

To determine the rheological properties of these solutions, a Haake Rotovisco RV20 viscometer was used to measure the fluid viscosity and a Rheometrics RMS-605 rheometer was used to detect the first normal stress of the coating solutions. If a test solution exhibited the shear-thinning behavior, we used the power-law model, i.e.,

$$\tau = \mu\dot{\gamma} = k\dot{\gamma}^n \qquad (1)$$

or

$$\mu = k\dot{\gamma}^{n-1} \qquad (2)$$

to represent the fluid viscosity.

The surface tension of these test fluids was measured by a CBVP-A3 surface tensometer (Kyowa Kaimenkagula Co., Japan) and the fluid density was determined by a pycnometer. The physical properties of all the test coating solutions are listed in Table I.

The top three solutions in Table I exhibited shear-thinning behavior, and the material constants k and n were estimated from the viscosity data. The first normal stress of the top two solutions could not be detected by the RMS rheometer; therefore, we consider these two solutions as standard inelastic power-law fluids. For the third solution, it showed minor shear-thinning behavior, i.e., its power-law index n was close to 1, but this fluid was elastic. Therefore, it can be considered as a Boger fluid,[28] which is an elastic fluid with constant viscosity. Since the viscosity of this solution was almost constant, the effect of fluid elasticity could be separated from the effect caused by viscosity variations and studied independently. The rheological properties of this solution

Table I   Physical Properties of Test Fluids

Test Fluids	Viscosity (Pa s)		Surface Tension (dyn/cm)	Density (g/cm^3)
	n	k		
Power-law fluids				
0.12% CMC/glycerine/water	0.86	0.206	66.0	1.20
2% PIB/kerosene/decalin	0.74	0.325	25.0	0.92
Boger fluid				
0.77% PIB/kerosene/PB	0.93	2.335	30.0	0.89
Newtonian fluids				
Silicone oil				
TSF-10		0.010	22.0	0.96
TSF-50		0.050	22.0	0.96
TSF-100		0.100	22.0	0.96
TSF-350		0.350	22.0	0.96
TSF-1000		1.000	22.0	0.96
PB		1.765	29.5	0.91
5% Decalin/PB		0.344	29.0	0.91
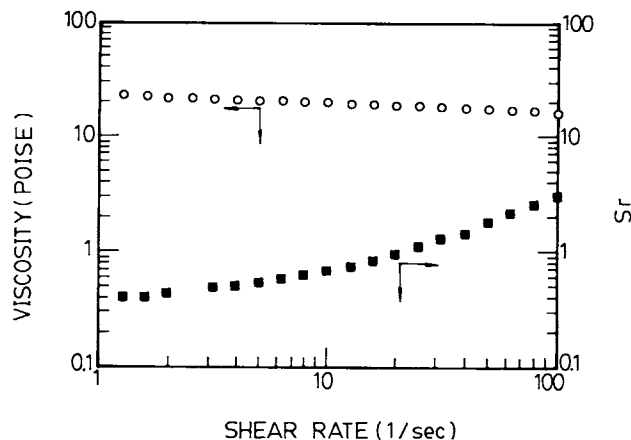
Figure 2 The rheological properties of the PIB/PB solution.

are shown in Figure 2. Note that a stress ratio (or recoverable shear) Sr is defined as

$$\text{Sr} \equiv N_1/2\tau \tag{3}$$

to represent the fluid elasticity.

RESULTS AND DISCUSSION

We first discuss the results of the forward coating system. Coyle[23] analyzed the coating flow of a similar system for Newtonian fluids experimentally and also proposed a theoretical model[24] to include the effect of roll deformation. He developed two equations to predict the coating thickness:

(a) Equation based on data correlation

$$T \sim (\mu V)^{0.49} W^{-0.43} E^{-0.41} R^{0.42} \tag{4}$$

(b) Equation based on the theoretical model

$$T \sim (\mu V)^{0.5} W^{-0.167} E^{-0.33} R^{0.4} \tag{5}$$

Apparently there are discrepancies, particularly in the effect of roll deformation, between these two equations.

We started the experiment with Newtonian fluids; besides the fluid viscosity and roll speed, the effect of the hardness of the deformable roll and the deflection length were also examined. The operating ranges of these parameters are given in Table II.

The effect of fluid viscosity and the hardness of the deformable roll on the coating thickness T_2 are shown in Figure 3. Note that the experiment was

Table II Range of Operation Variables

|	Roll Speed (cm/s)	Speed Ratio (V_2/V_1)	Defection Length (mm)
Forward coating	14–150	0.7–2.0	0.05–0.2
Reverse coating	14–90	0.2–11	0.05–1.4

performed with the two rolls moving at the same speed. Generally, as the roll speed goes up, the coating thickness will increase, and this trend is more significant if the deformable roll is softer. The fluid viscosity tends to resist the pressing force of the deformable roll; therefore, the higher the fluid viscosity, the thicker the coating thickness.

The effect of the deflection length H_0 for three Newtonian solutions on the coating thickness T_2 is shown in Figure 4. T_2 can be reduced by pressing the deformable roll harder, or by increasing H_0. However, this effect is less significant as H_0 keeps going up and T_2 tends to approach a constant value as H_0 is greater than 1.0 mm for these solutions.

We also developed an empirical equation for coating thickness through a least-square procedure:

$$T_2 \sim (\mu V)^{0.5} H_0^{-0.47} E^{-1.6} \tag{6}$$

A comparison of the prediction of eq. (6) with the experimental data is given in Figure 5; the solid line represents the prediction of eq. (6), and the fit appears to be acceptable.

V (cm/sec)
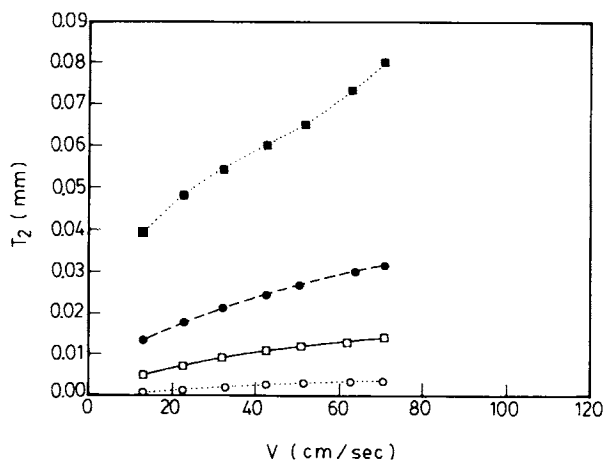
Figure 3 Forward coating: the effect of fluid viscosity and roll hardness on the coating thickness. $H_0 = 0.3$ mm. (●) $\mu = 0.1$ Pa s, Hs = 60; (○) $\mu = 0.1$ Pa s, Hs = 90; (■) $\mu = 1.0$ Pa s, Hs = 60; (□) $\mu = 1.0$ Pa s, Hs = 90.
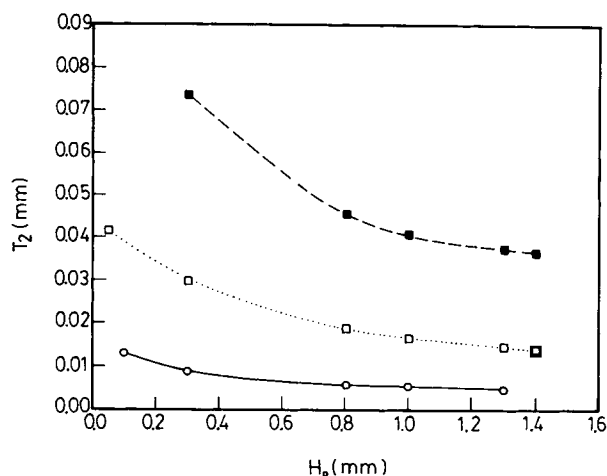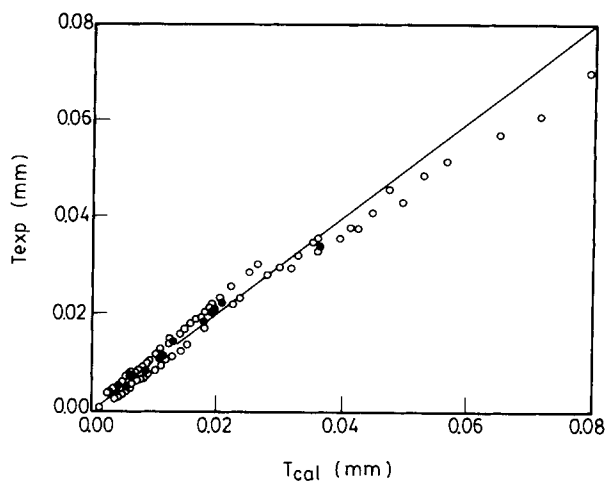
Figure 4 Forward coating: the effect of deflection length H_0 on the coating thickness. $V = 62$ cm/s, Hs = 60. μ (Pa s): (O) 0.01; ($\square$) 0.1; ($\blacksquare$) 1.0.

Figure 5 Forward coating: comparison of the prediction of eq. (6) with the experimental data: (O) data for two rolls with equal speed; ($\bullet$) data for two rolls at different speeds.

Comparing eq. (6) with the equations of Coyle, we note that the dependence of (μV) is in good agreement; therefore, the experimental observation by Coyle on the effect of (μV) is verified. However, the effect of the hardness of deformable rolls is quite different; this may be due to the fact that deformable rolls used in Coyle's and our experiments do not have the same dimensions and physical properties. Therefore, the effects of Young's modulus and other variables are system-dependent.

Equation (6) is based on the experimental data for two rolls that move at the same speed. We also performed some experiments with rolls moving at different speeds. It was found that eq. (6) is still valid for rolls moving at different speeds if we replace the speed V by the average speed $(V_1 + V_2)/2$. A comparison of eq. (6) with the experimental data is also shown in Figure 5; the solid line represents the prediction of eq. (6), it is clear that, within the range of our experimental condition, the fit is reasonably good.

We also checked the fluid distribution on the two rolls at different speed ratios. The results for three Newtonian fluids are shown in Figure 6; the solid line represents a situation where an equal amount of coating solution is deposited on both rolls. It is noted that even when the two rolls moved at different speeds, the liquid films coated on the rolls had relatively equal thickness.
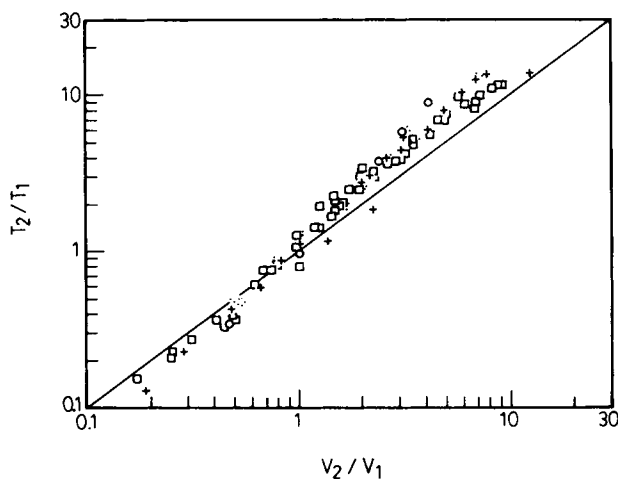
The coating thickness for two shear-thinning fluids is shown in Figure 7. The experimental results for two Newtonian fluids are also plotted in this figure for comparison. It is interesting to note that the apparent viscosities of these two solutions are

higher than 0.1 Pa s at low shear rates; however, owing to the shear-thinning behavior, the coating thickness is less than that of the 0.1 Pa s Newtonian solution. For the solution with a higher degree of shear-thinning, i.e., the solution with $n = 0.75$, the coating thickness is even lower than a 0.01 Pa s solution. Similar results for a smaller deflection length H_0 are given in Figure 8.

Since the coating solution has to pass a narrow channel between the rigid and deformable rolls, the shear rates in the channel are high, and, consequently, for a shear-thinning fluid, its apparent viscosity is drastically reduced. As we have learned from

Figure 6 Forward coating: the ratio of coating thickness as a function of speed ratio: ($\square$) $\mu = 0.01$ Pa s; (+) $\mu = 0.1$ Pa s; (O) $\mu = 1.0$ Pa s.
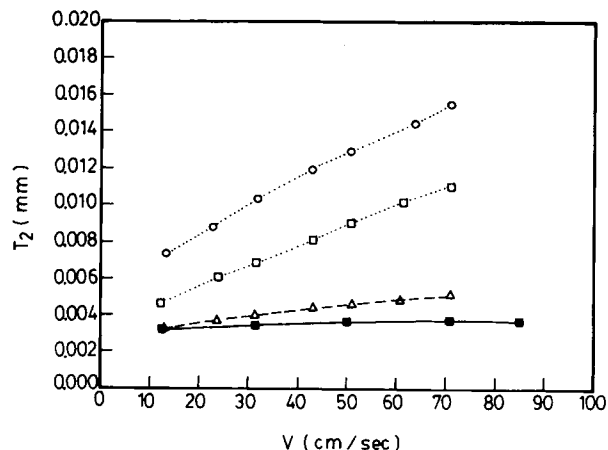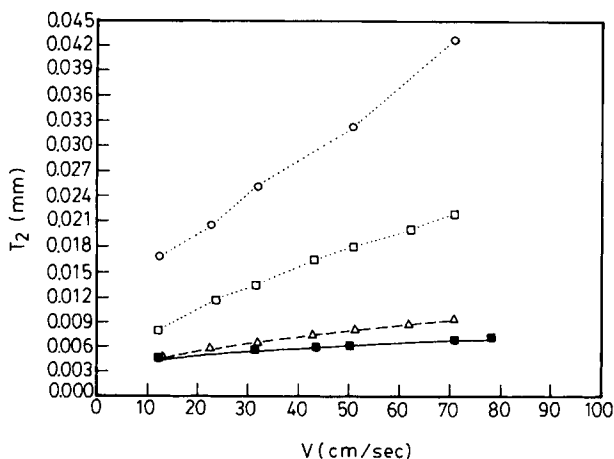
Figure 7 Forward coating: the effect of shear-thinning behavior on the coating thickness for H_0 = 1.3 mm, Hs = 60: ($\triangle$): μ = 0.01 Pa s; ($\bigcirc$) μ = 0.1 Pa s; ($\square$) k = 0.206 Pa s^n, n = 0.86; ($\blacksquare$) k = 0.324 Pa s^n, n = 0.75.

the results of Newtonian coating flow, lowering fluid viscosity can decrease the coating thickness; hence the shear-thinning behavior of the fluid will reduce the coating thickness. The gap of the narrow channel is very difficult to measure, if we take the coating thickness T_2 as the characteristic length and estimate the apparent viscosity of a shear-thinning fluid as follows,
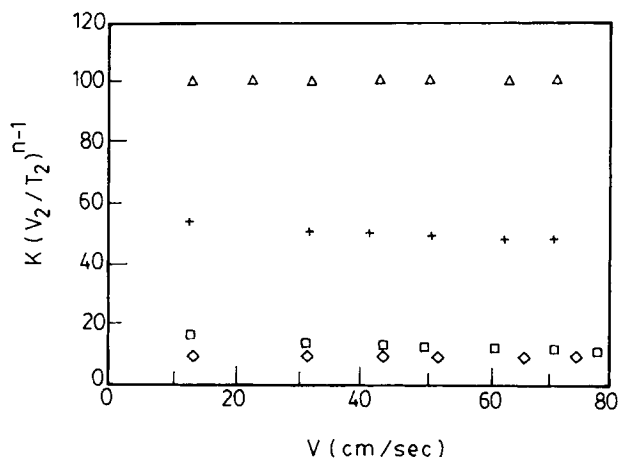
$$\mu = k(V_2/T_2)^{n-1} \qquad (7)$$

then the apparent viscosities for the two shear-thinning fluids at different coating speeds can be approximated. The apparent viscosities corresponding

to different coating speeds in Figure 7 are plotted in Figure 9. The results indicate that the apparent viscosities drop gradually as the coating speed goes up. It should be noted that the channel gap between the two rolls is smaller than the coating thickness, the viscosity data in Figure 9 can only be considered as a reference for comparison, and the fluid apparent viscosities in the channel should be lower than the values presented in Figure 9.

The effect of fluid elasticity can be demonstrated by the results in Figure 10. The coating thickness of the Newtonian PB solution increases as the coating speed goes up. After adding a small amount of PIB, the PIB/PB solution becomes slightly shear-thinning (n = 0.93), but the viscosity remains close to the pure PB solution at different shear rates. We observed that lateral waves appeared at coating speed lower than 10 cm/s for the PIB/PB solution. Therefore the coating thickness T_2 for this solution in Figure 10 is actually an average thickness for the wavy film. The normal forces exerted by the elastic fluid on the two rolls in the nip region will enlarge the channel gap between the two rolls, and, consequently, the coating thickness of the PIB/PB solution is much higher than that of the pure PB solution. The phenomenon of ribbing becomes more severe as the coating speed goes up and finally the liquid film on the roll surface breaks into many ribs as shown in Figure 11; it is meaningless to determine the coating thickness under this condition. This explains why no data point is presented for the PIB/PB solution at coating speed 70 cm/s in Figure 10. Our observation of the elastic effect is consistent with the work of Bauman et al.[13] on two rigid rolls:

Figure 8 Forward coating: the effect of shear-thinning behavior on the coating thickness for H_0 = 0.3 mm, Hs = 60: ($\triangle$) μ = 0.01 Pa s; ($\bigcirc$) μ = 0.1 Pa s; ($\square$) k = 0.206 Pa s^n, n = 0.86; ($\blacksquare$) k = 0.324 Pa s^n, n = 0.75.

Figure 9 Forward coating: estimated apparent viscosities as a function of the coating speed: ($\diamond$) μ = 0.01 Pa s; ($\triangle$) μ = 0.1 Pa s; (+) k = 0.206 Pa s^n, n = 0.86; ($\square$) k = 0.324 Pa s^n, n = 0.75.
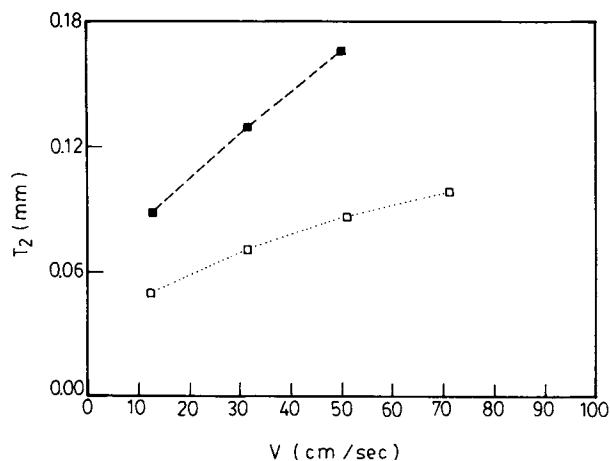
Figure 10   Forward coating: the effect of fluid elasticity on the coating thickness. $H_0 = 0.3$ mm, Hs $= 60$: ($\square$) μ $= 1.765$ Pa s; ($\blacksquare$) $k = 2.336$ Pa s^n, $n = 0.93$.

They also found that the fluid elasticity destabilizes the coating flow in a forward coating operation.

The major function of the rolls in the reverse coating system in Figure 1(b) is to transfer a uniform liquid film from roll R_1 to roll R_2 smoothly. Booth[2] called the speed ratio (V_2/V_1) that transfers the liquid film without defects the "wipe ratio." He stated that the wipe ratio for most coating systems was between 0.6 and 4.

The ranges of operating variables in the reverse coating experiment are given in Table II. We used
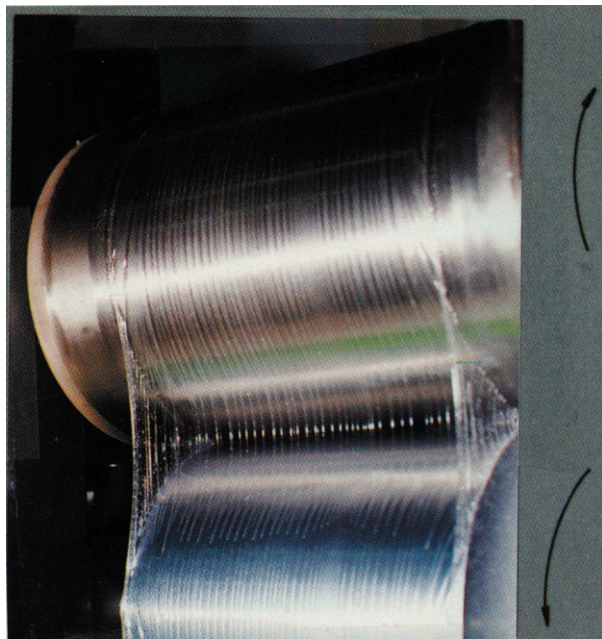
**Figure 11**   Forward coating: flow instability caused by fluid elasticity.
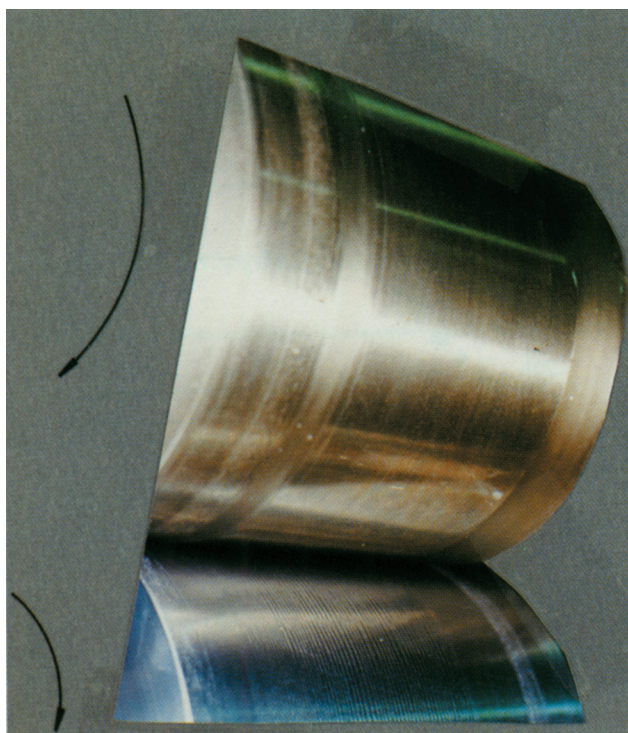
Figure 12   Reverse coating: ribbing on roll R_2.

a T-die to deliver a uniform liquid film on the surface of roll R_1. Since the flow rate through a T-die could be measured accurately, the coating thickness on R_1 could be estimated easily. To determine the wipe ratio, we fixed the speed of R_1. After a uniform liquid film was transferred onto the surface of R_2 without defect, we started increasing the speed of R_2 until ribs, as shown in Figure 12, appeared on the liquid film surface; then we could determine the wipe ratio (V_2/V_1) for the onset of ribbing.

The effect of liquid film thickness T_1 on the critical speed V_2 for a Newtonian solution is shown in Figure 13. Ribbing would appear if the speed of R_2 is higher than the value of V_2 in the figure. It is clear that the liquid film thickness T_1 has little effect on the wipe ratio. The effect of Newtonian viscosity on the critical speed V_2 is also given in Figure 13. Similarly the fluid viscosity has little effect on the wipe ratio.

We also examined the relationship between the wipe ratio (V_2/V_1) and the capillary number Ca $\equiv$ $\mu V_1/\sigma$ for the Newtonian coating experiment. It appears that this ratio is independent of Ca and through a least-square procedure, the value 1.2 was found as the wipe ratio for Newtonian fluids.

The effect of polymer additives on the critical speed V_2 is shown in Figure 14. The solid line represents the Newtonian wipe ratio 1.2. Three polymer solutions were used. It is interesting to note that V_2
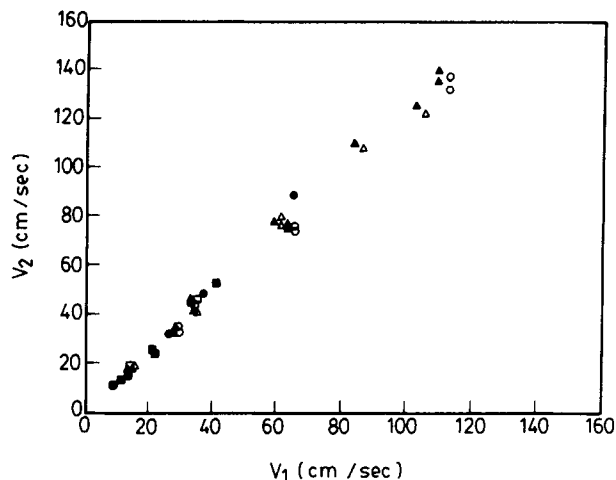
Figure 13 Reverse coating: critical speed V_2 as a function of the film thickness T_1: (a) $\mu = 0.1$ Pa s; (○) T_1 = 0.065 mm; (□) T_1 = 0.3 mm; (△) T_1 = 0.12 mm; (b) T_1 = 0.12 mm; (●) $\mu = 0.01$ Pa s; (■) $\mu = 0.1$ Pa s; (▲) $\mu = 1.0$ Pa s.

can be increased slightly by adding polymers to coating solutions, that the average wipe ratio for these polymer solutions is 1.6, and that the contribution of the shear-thinning and elastic behavior is indistinguishable.

Similar stabilizing effects of polymer additives for coating flows were observed by Guttof and Kendrick[25] for slide coating and by Lee[26] for extrusion coating. Examining these three types of coating flows, we note that coating solutions only change flow directions in the bead region as shown in Figure
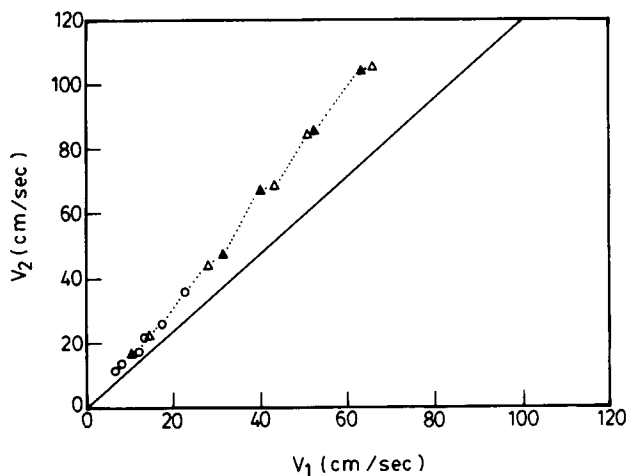

Figure 14 Reverse coating: wipe ratio for three polymer solutions: (▲) 0.12% CMC/glycerine/water; (△) 2% PIB/kerosene/decalin; (○) 0.77% PIB/kerosene/PB (Boger fluid); (———) Newtonian fluids.

15, and long-chain molecules of polymer additives tend to stabilize the coating bead as the coating speed goes up and postpone the ribbing. On the other hand, if the coating system has a diverging flow field such as the forward roll coating in Figure 15, polymer solutions with significant elastic behavior may destabilize the flow field and the onset of ribbing would occur at a lower coating speed.

CONCLUSION

We have examined the effect of polymer additives on the performance of a two-roll coater, one being a rigid roll and the other a deformable roll. Both forward and reverse coating operations have been analyzed.

For the forward coating system, we have confirmed some of the experimental results of Coyle for Newtonian fluids, and found that the shear-thinning behavior of the polymer coating solution can reduce the coating thickness; but if the polymer coating solution exhibits significant elastic behavior, the
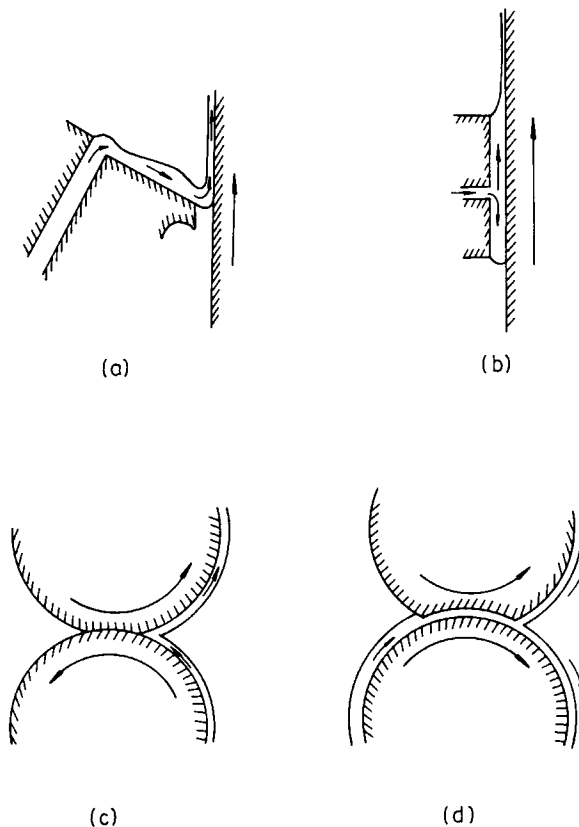
Figure 15 Flow directions in various coating operations: (a) slide coating; (b) extrusion coating; (c) reverse roll coating; (d) forward roll coating.

normal forces exerted on the roll surfaces will enlarge the channel gap in the nip region and increase the coating thickness. The elastic effect can also destabilize the coating flow and the onset of ribbing will occur at a lower coating speed.

For the reverse coating system, the wipe ratio for Newtonian solutions was found to be 1.2. With polymer additives, this ratio can go up to 1.6, irrespective of the rheological properties of the polymer solutions.

We conclude that the elastic effect of polymer additives may destabilize the coating flow if the flow field has a diverging geometry, but the long-chain molecules of polymers may stabilize the coating flow if the flow only changes directions.

NOMENCLATURE

Ca	capillary number, $\mu V_1/\sigma$
E	Young's modulus of the deformable roll
H_0	deflection length of the deformable roll defined in Figure 1
Hs	hardness of the deformable roll
k	material constant of the power-law model
N_1	first normal stress difference
n	power-law index
R	radius of the roll
R_1	radius of the rigid roll
R_2	radius of the deformable roll
Sr	a stress ratio defined in eq. (3)
T	coating thickness
T_1	coating thickness on the rigid roll
T_2	coating thickness on the deformable roll
T_{cal}	average coating thickness predicted by eq. (6)
T_{exp}	average experimental coating thickness, $(T_1 + T_2)/2$
V	coating speed
V_1	coating speed of the rigid roll
V_2	coating speed of the deformable roll
W	applied force on the roll

Greek Letters

$\dot\gamma$	shear rate
μ	fluid viscosity
ρ	density
σ	surface tension
τ	shear stress

REFERENCES

1. K. J. Ruschak, *Ann. Rev. Fluid Mech.*, **17**, 65 (1985).
2. G. L. Booth, *Coating Equipment and Processes*, Lockwood, New York, 1970.
3. E. Pitts and J. Greiller, *J. Fluid Mech.*, **11**, 33 (1961).
4. C. C. Mill and G. R. South, *J. Fluid Mech.*, **28**, 523 (1967).
5. J. Greener and S. Middleman, *Polym. Eng. Sci.*, **15**, 1 (1975).
6. J. Greener and S. Middleman, *Ind. Eng. Chem. Fundam.*, **18**, 35 (1979).
7. J. Greener, T. Sullivan, B. Turner, and S. Middleman, *Chem. Eng. Commun.*, **5**, 73 (1980).
8. H. Benkreira, M. F. Edwards, and W. L. Wilkinson, *Chem. Eng. Sci.*, **36**, 423 (1981).
9. H. Benkreira, M. F. Edwards, and W. L. Wilkinson, *Chem. Eng. Sci.*, **36**, 429 (1981).
10. H. Benkreira, M. F. Edwards, and W. L. Wilkinson, *Chem. Eng. J.*, **25**, 211 (1982).
11. K. J. Ruschak, *J. Fluid Mech.*, **119**, 107 (1982).
12. M. D. Savage, *J. Fluid. Mech.*, **117**, 443 (1982).
13. T. Bauman, T. Sullivan, and S. Middleman, *Chem. Eng. Commun.*, **14**, 35 (1982).
14. M. D. Savage, *J. Appl. Math. Phys.*, **34**, 358 (1983).
15. M. D. Savage, *AIChE J.*, **30**, 999 (1984).
16. H. Benkreira, M. F. Edwards, and W. L. Wilkinson, *J. Non-Newtonian Fluid Mech.*, **14**, 377 (1984).
17. D. J. Coyle, C. W. Macosko, and L. E. Scriven, *J. Fluid Mech.*, **171**, 183 (1986).
18. D. J. Coyle, C. W. Macosko, and L. E. Scriven, *AIChE J.*, **33**, 741 (1987).
19. D. A. Soules, R. H. Fernando, and J. E. Glass, *J. Rheol.*, **32**, 181 (1988).
20. J. Greener and S. Middleman, *Ind. Eng. Chem. Fundam.*, **20**, 63 (1981).
21. H. Benekreira, M. F. Edwards, and W. L. Wilkinson, *Chem. Eng. Sci.*, **37**, 277 (1982).
22. D. J. Coyle, C. W. Macosko, and L. E. Scriven, *AIChE J.*, **36**, 161 (1990).
23. D. J. Coyle, *AIChE Spring National Meeting*, New Orleans, LA, March, 1988.
24. D. J. Coyle, *Chem. Eng. Sci.*, **43**, 2673 (1988).
25. E. B. Guttoff and C. E. Kendrick, *AIChE J.*, **28**, 459 (1982).
26. K. Y. Lee, *PhD. thesis*, National Tsing Hua University, Taiwan, 1990.
27. K. Y. Lee and T. J. Liu, *Polym. Eng. Sci.*, **29**, 1056 (1989).
28. R. J. Binnington and D. V. Boger, *Polym. Eng. Sci.*, **26**, 133 (1986).